Available online at www.sciencedirect.com
SCIENCE DIRECT®
Solar Energy Materials & Solar Cells
ELSEVIER
Solar Energy Materials & Solar Cells 87 (2005) 395–409
www.elsevier.com/locate/solmat

Enhancing solar cell efficiency by using spectral converters

W.G.J.H.M. van Sark[a,*], A. Meijerink[b], R.E.I. Schropp[c], J.A.M. van Roosmalen[d], E.H. Lysen[e]

[a]*Department of Science, Technology and Society, Copernicus Institute, Utrecht University, Heidelberglaan 2, 3584 CS Utrecht, the Netherlands*
[b]*Department of Chemistry of Condensed Matter, Debye Institute, Utrecht University, Princetonplein 5, 3584 CC Utrecht, the Netherlands*
[c]*Department of Surfaces, Interfaces and Devices, Debye Institute, Utrecht University, Padualaan 8, 3584 CH Utrecht, the Netherlands*
[d]*ECN Solar Energy, P.O. Box 1, 1755 ZG Petten, the Netherlands*
[e]*Utrecht Centre for Energy research (UCE), Utrecht University, Heidelberglaan 2, 3584 CS Utrecht, the Netherlands*

Received 15 May 2004; received in revised form 5 July 2004; accepted 8 July 2004
Available online 2 December 2004

Abstract

Planar converters containing quantum dots as wavelength-shifting moieties on top of a multi-crystalline silicon and an amorphous silicon solar cell were studied. The highly efficient quantum dots are to shift the wavelengths where the spectral response of the solar cell is low to wavelengths where the spectral response is high, in order to improve the conversion efficiency of the solar cell. It was calculated that quantum dots with an emission at 603 nm increase the multi-crystalline solar cell short-circuit current by nearly 10%. Simulation results for planar converters on hydrogenated amorphous silicon solar cells show no beneficial effects, due to the high spectral response at low wavelength.

Keywords: Efficiency; Spectral converters

*Corresponding author. Tel.: +31 30 253 7611; fax: +31 30 253 7601.
E-mail address: w.g.j.h.m.vansark@chem.uu.nl (W.G.J.H.M. van Sark).

0927-0248/$ - see front matter © 2004 Elsevier B.V. All rights reserved.
doi:10.1016/j.solmat.2004.07.055

1. Introduction

Conventional single-junction semiconductor solar cells only effectively convert photons of energy close to the semiconductor band gap E_g as a result of the mismatch between the incident solar spectrum and the spectral absorption properties of the material [1,2]. Photons with energy E_{ph} smaller than the band gap are absorbed and their energy is totally wasted. Photons with energy E_{ph} larger than the band gap are absorbed, but the excess energy $E_{ph}-E_g$ is not used effectively due to thermalization of the electrons. These fundamental spectral losses in a single-junction silicon solar cell can be as large as 50%. Several routes have been proposed to overcome this drawback, and all of these methods or concepts concentrate on a better exploitation of the solar spectrum, e.g., intermediate band gaps [3], quantum dot concentrators [4] and down- and up-converters [5,6]. They are in general referred to as Third Generation (3G) photovoltaics [7,8]. The recently started European project FULLSPECTRUM aims to better use the full solar spectrum by further developing concepts already scientifically proven but not yet developed, and by trying to prove new ones in the search for a breakthrough in PV technology [9].

Single-junction solar cells optimally perform under monochromatic light of a wavelength λ_{opt}: $1240/E_g$. A monochromatic solar cell can in principle reach efficiencies over 80%, which is slightly dependent on band gap [10]. For (multi)crystalline silicon (mc-Si) solar cells $\lambda_{opt} = 1100\,\text{nm}$ (with $E_g = 1.1\,\text{eV}$); for hydrogenated amorphous silicon (a-Si:H) the optimum wavelength is $\lambda_{opt} = 700\,\text{nm}$ (with $E_g = 1.77\,\text{eV}$). As amorphous silicon solar cells only contain a thin absorber layer, the optimum spectrum response occurs at about 550 nm [11,12]. The conversion efficiency of these types of cells measured at incident monochromatic light of 550 nm can be as high as 20%, in contrast to the observed AM1.5G efficiency of 10% [13].

Conversion of the incident solar spectrum to monochromatic light would greatly increase the observed efficiency [10]. To this end, one needs to convert the energy of incident photons such that E_{ph} equals E_g, or is slightly larger. This involves down conversion (exactly one high-energy photon is converted to exactly two lower energy photons) and up conversion (exactly two low-energy photons are converted to exactly one higher energy photon) [5,6]. To distinguish any modification of photon energy from these distinct terms down and up conversion, the term *spectral* down conversion (SDC) or *spectral* up conversion (SUC) is more general.

Spectral down conversion was suggested in the 1970s to be used in so-called luminescent concentrators that were attached on to a solar cell [14–17]. In these concentrators, organic dye molecules absorb incident light and re-emit this at a red-shifted wavelength. Internal reflection ensures collection of all the re-emitted light in the underlying solar cells. As the spectral sensitivity of silicon is higher in the red than in the blue, an increase in solar cell efficiency was expected. Also, it was suggested to use a number of different organic dye molecules of which the re-emitted light was matched for optimal conversion by different solar cells. This is similar to using a stack of multiple solar cells, each sensitive to a different part of the solar spectrum. The expected high efficiency in practice was not reached as a result of not

being able to meet the stringent requirements to the organic dye molecules, such as high quantum efficiency and stability, and the transparency of collector materials in which the dye molecules were dispersed [14–17].

Research in this field was revitalized recently through the development of the quantum dot concentrator [4,18,19]. Quantum dots (QDs) were proposed for use in luminescent concentrators instead of organic dye molecules. QDs are nanometer-sized semiconductor crystals of which the emission wavelength can be tuned by their size, as a result of quantum confinement [20,21]. The advantages of QDs with respect to organic dye molecules are their high brightness, stability and quantum efficiency [22]. Quantum dots absorb all the light of a wavelength smaller than the absorption maximum $(\approx E_g)$, in contrast to the small-band absorption of dye molecules. As an example, CdSe/ZnS core-shell QDs of 4 nm diameter have an emission maximum around 550 nm [23–25], which would be ideally suited for amorphous silicon solar cells.

A simple and potentially cheap way of employing the principle of SDC for solar cells is to coat them with a transparent layer that contains a spectrum-shifting moiety. Such a planar spectral down converter can be applied to existing solar cells without modifications to the solar cell design. Hence, optimization of the converter to yield an increase in the conversion efficiency of the solar cell can be done independently of the solar cell. Few have reported recently on increases in conversion efficiency: an 8% relative increase in conversion efficiency was reported in case of a CdS/CdTe solar cell, where the coating in which a fluorescent coloring agent was introduced increased the sensitivity in the blue [26]. Other showed results that indicate a 6% relative increase in conversion efficiency [27] upon coating a multi-crystalline silicon solar cell. The employed luminescent species has an absorption band around 400 nm and a broad emission between 450 and 550 nm. As QDs have a much broader absorption it is expected that in potential the deployment of QDs in planar converters could lead to relative efficiency increases of 20–30%. Spectral down conversion employing QDs in a polymer composite has been demonstrated in a light-emitting diode (LED), where a GaN LED was used as an excitation source ($\lambda_{em} = 425$ nm) for QDs emitting at 590 nm [28]. Besides QDs, other materials have been suggested such as rare-earth ions [29] and dendrimers [30]. A maximum increase of 22.8% was calculated for a thin film coating of $KMgF_3$ doped with Sm on top of a CdS/CdTe solar cell, while experimental results show an increase of 5% [31].

In this paper, we will explore the feasibility of QD use in planar converters on top of solar cells. First, a quick method is used to assess the effects of varying emission wavelength on solar cell performance using small-band QD emission spectra. Second, a more detailed method is used, where the effect of the incorporation of QDs in a plastic layer on the incident solar spectrum is determined. This includes different QD sizes (i.e., absorption/emission maxima) and concentrations. The modified spectrum then is used as input in solar cell simulation programs suited for either crystalline or amorphous silicon. We will study the effects of QD size (spectral properties) and concentration on the conversion efficiency and will determine the optimum for both the mc-Si and a-Si:H solar cell. As the spectral response of these

types of cells differs, we expect that also the optimum combination of QD size and concentration differ.

2. Methodology

The configuration that is studied is depicted in Fig. 1. A plastic layer containing quantum dots is applied on top of a solar cell. The size of the quantum dots is chosen such that their emission maximum is in the red part of the spectrum; they thus will absorb both blue as well as green incident light. We implicitly assume that the solar cell has an optimum spectral response in the red. Depending on the concentration of QDs also unabsorbed blue and green light enters the solar cell. Of course, highly transparent plastics are to be used.

The effects of QDs in planar converters will be assessed on standard baseline solar cells that are reproducibly manufactured at ECN and Utrecht University. We will first describe the two types of solar cells under investigation, i.e., multi-crystalline silicon and hydrogenated amorphous silicon. Their performance will be simulated under standard AM1.5G spectral conditions using software specifically designed for either material.

Inclusion of QDs in a planar converter on top of a solar cell leads to spectral changes. We will first study the effect of small-band emission spectra of QDs on the solar cell performance parameters. This will quickly show the potential benefits of QD use. Finally, a more thorough analysis will be carried out that includes the modifications of the AM1.5G spectrum due to QD absorption and emission.

2.1. Solar cell configurations

The standard baseline n–p–p^+ mc-Si cell has parameters that are typical of low-cost commercial products, including series resistance, shunt conductance and a second diode [32]. It measures $10 \times 10\,cm^2$ in area, has a thickness of 300 μm, and has a shallow diffused emitter of 50 Ω/sq. The front broadband reflectance is 9% across

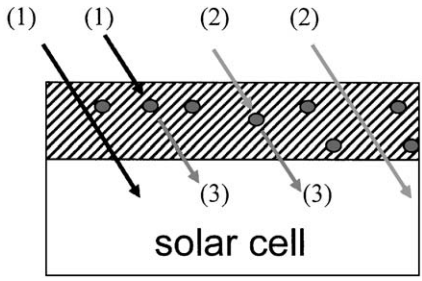

Fig. 1. Schematic drawing of the studied configuration. A plastic layer containing quantum dots is applied on top of a solar cell. Both blue (1) and green (2) light are absorbed by the quantum dot and re-emitted in the red (3), which is subsequently absorbed in the solar cell. Also, unabsorbed blue and green light enters the solar cell as well.

the solar spectrum, as a result of the front surface anti-reflection coating (71-nm thick silicon nitride with a refractive index $n = 2.1$). The thickness of the back-surface field (BSF) is 9 μm and has a p^+ doping level of $4 \times 10^{18}\,cm^{-3}$. The performance of the solar cell is simulated with the simulation programme PC1D (version 5.8) [33,34]. The calculated performance parameters (short-circuit current I_{sc}, open-circuit voltage V_{oc}, fill factor FF, efficiency η) are given in Table 1; the current–voltage (IV) characteristics and spectral response are shown in Fig. 2.

The standard baseline a-Si:H cell has the usual layer configuration glass/TCO/*p*-a-SiC:H/*i*a-Si:H/*n* a:Si:H/Ag, with layer thicknesses of 1 mm, 1 μm, 8, 500, 20, and 200 nm, respectively [11]. TCO is a transparent conductive coating, such as SnO_2. Activation energies for n and p layer are 0.24 and 0.46 eV, respectively. Solar cell performance is simulated with the programme ASA (version 3.3) that includes specific features of amorphous semiconductors, such as sloped band edges and mid-gap dangling bond density models [11,35]. The calculated performance is compared to the performance of the mc-Si cell in Table 1 and Fig. 2.

2.2. Small-band spectrum

A simple approach that allows the selection of the most appropriate QD size entails simulation of solar cell performance employing small-band QD emission spectra solely. To this end, we used normalized emission spectra and scaled them such that the integrated spectral density was $500\,W/m^2$. A typical normalized emission spectrum is shown in Fig. 3 [36]. These scaled spectra were then used as input for the simulation programmes PC1D and ASA. We varied the center emission wavelengths in 50-nm steps in the range 400–1000 nm, and simulated solar cell performance.

2.3. Modified AM1.5G spectrum

In the configuration shown in Fig. 1, the incident AM1.5G spectrum converted to amount of photons per wavelength $\Phi_s(\lambda)$ will be modified by absorption of photons. First, the amount of absorbed photons $\Phi_a(\lambda)$ is determined from the QD absorption spectrum, which depends on the QD size, their concentration in the converter layer, and the thickness of this layer. This absorbed amount is subtracted from the

Table 1
Solar cell performance parameters calculated with PC1D (mc-Si) and ASA (a-Si:H)

	mc-Si	a-Si:H
$I_{sc}(mA/cm^2)$	31.19	11.92
$V_{oc}(V)$	0.6028	0.8135
FF	0.7707	0.6753
η (%)	14.49	6.548

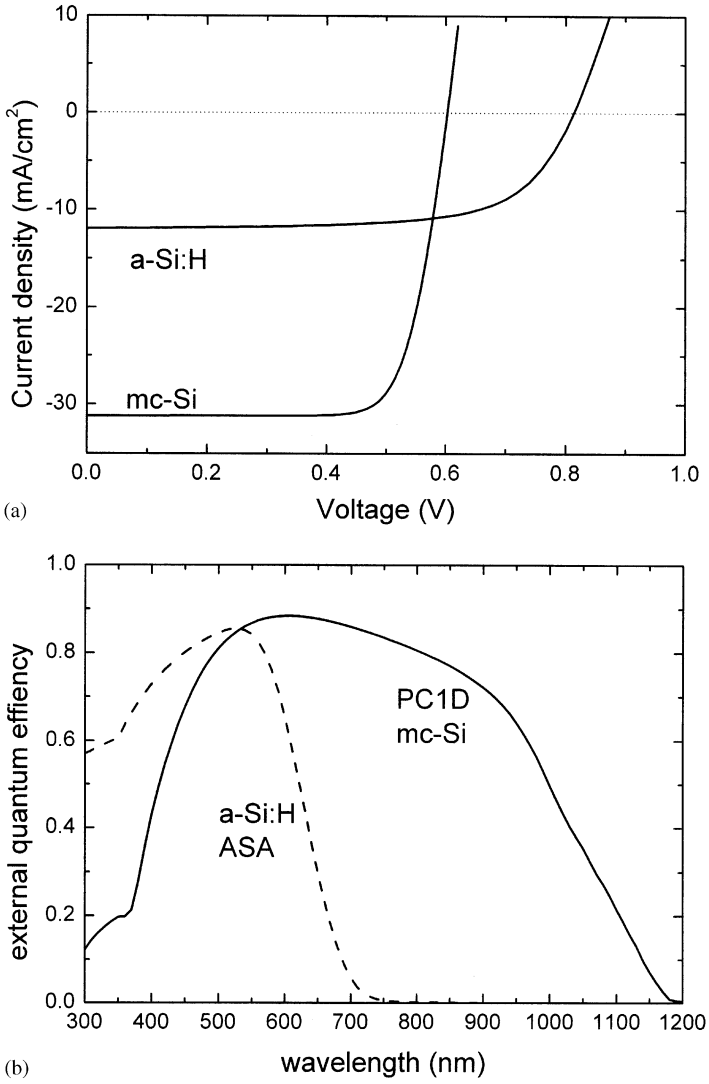

Fig. 2. Performance of the two solar cells, mc-Si and a-Si:H. (a) current–voltage characteristics; (b) spectral response.

AM1.5G spectrum:

$$\Phi_{sa}(\lambda) = \Phi_s(\lambda) - \Phi_a(\lambda). \tag{1}$$

As the QDs re-emit light at a red-shifted wavelength, the amount of emitted photons $\Phi_e(\lambda)$ is calculated from the QD emission spectrum. To this end, data for quantum efficiency is assumed, as well as the assumption that $\frac{3}{4}$ of the emitted photons is

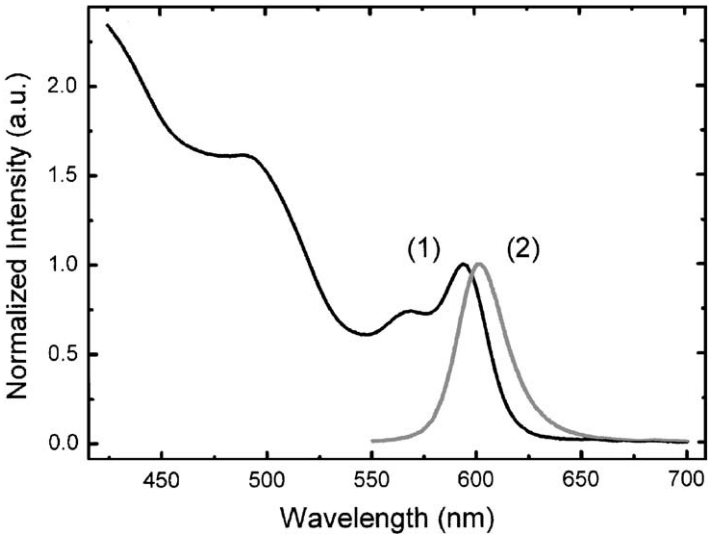

Fig. 3. Normalized absorption (1) and emission (2) spectrum of CdSe nanocrystals of 4.3 diameter, capped with TOPO/TOP/HDA (data from S.F. Wuister (2003), see also Ref. [30]).

directed towards the underlying solar cell, due to internal reflection in the converter layer [19].

The amount of emitted photons then is added to the already modified AM1.5G spectrum:

$$\Phi_{\mathrm{sa\,e}}(\lambda) = \Phi_{\mathrm{sa}}(\lambda) + \Phi_{\mathrm{e}}(\lambda). \tag{2}$$

Finally, the resulting spectrum serves as input for the solar cell simulation models.

The most common approach to calculate absorption of photons is by using the Lambert–Beer equation: the photon flux density $\Phi(x,\lambda)$ after passing a distance x in a film with absorption coefficient $\alpha(\lambda)$ is reduced with a factor $\exp(-\alpha(\lambda)x)$, which can be written as

$$\Phi(x,\lambda) = \Phi^0(\lambda)\exp(-\alpha(\lambda)x), \tag{3}$$

where $\Phi^0(\lambda)$ is the incident photon flux density. The exponential term equals $\alpha(\lambda)x = \varepsilon_\lambda CD$, with ε_λ the molar extinction coefficient ($\mathrm{M^{-1}\,cm^{-1}}$), C the chromophore concentration (M), and D the thickness of the film (cm). The molar extinction coefficient can be measured directly, or determined from measurement of the absorption spectrum (see below). The chromophore or QD concentration can be varied at will, from the nM to the mM range. The thickness of the film (converter) typically will vary between about 1 μm and a few mm. In the following we will describe in detail the followed procedure for QDs emitting at 603 nm.

Quantum dots of high quantum yield ($\eta_{\mathrm{em}} = 0.8$) are routinely synthesized in our laboratory following a single-step route using trioctylphosphine oxide (TOPO) and hexadecylamine (HDA) [36]. The resulting typical (normalized) absorption $A_{\mathrm{n}}(\lambda)$

and emission $E_n(\lambda)$ spectra are shown in Fig. 3. These spectra have been normalized with respect to the absorption and emission maximum occurring at 594 and 603 nm, respectively. The normalized absorption spectrum can be converted to a wavelength-dependent molar extinction coefficient but requires the determination of the QD concentration with is cumbersome and time-consuming. Instead we used the reported cubic relationship between molar extinction coefficient and particle size as reported by Leatherdale et al. [37] (radius) and Schmelz et al. [38] (diameter). The particle diameter is determined from the absorption maximum at 594 nm using the relation between absorption maximum and particle diameter reported in literature [39–41], i.e., 4.24 nm in diameter. Thus, the QD radius a determined from experimental data is 2.12 nm. The absorption spectrum $A(\lambda)$ is scaled such that the molar extinction coefficient ε_λ at 350 nm equals $\varepsilon_\lambda(\mathrm{M^{-1}cm^{-1}}) = (1.438 \times 10^{26})a^3$, as reported by Leatherdale et al. [37]. The calculated ε_λ at 350 nm is $\varepsilon_{350} = 1.37 \times 10^6\,\mathrm{M^{-1}\,cm^{-1}}$. The data reported for the molar extinction coefficient by Schmelz et al. [38] give $\varepsilon_{602} = 2.65 \times 10^5\,\mathrm{M^{-1}\,cm^{-1}}$ for their 4.5 nm diameter CdSe particle. From their data one can infer that $\varepsilon_{602}/\varepsilon_{350} \approx 4.3$, so there is reasonable agreement with the data from Leatherdale et al. with only a difference of about 15% in ε_{350}.

The amount of absorbed photons $\Phi_{a,603}(D,\lambda)$ in the converter of thickness D and containing QDs of emission wavelength 603 nm now is

$$\Phi_{a,603}(D,\lambda) = \Phi_s(\lambda)\exp(-\varepsilon_\lambda CD) \tag{4}$$

and the modified amount $\Phi_{sa,603}(D,\lambda)$ is calculated with Eq. (1):

$$\Phi_{sa,603}(D,\lambda) = \Phi_s(\lambda) - \Phi_{a,603}(D,\lambda) = \Phi_s(\lambda)(1-\exp(-\varepsilon_\lambda CD)). \tag{5}$$

Now, photons will be emitted at quantum efficiency $\eta_{em} = 0.8$. Further assuming isotropic emission and internal reflection 75% of the emitted photons will reach the solar cell: $\eta_t = 0.75$. Therefore, the integrated amount of emitted photons equals $\eta_t\eta_{em}$ times the integrated amount of absorbed photons

$$\eta_t\eta_{em}\int \Phi_{a,603}(D,\lambda)\,d\lambda = \int \Phi_{e,603}(D,\lambda)\,d\lambda = k, \tag{6}$$

where $\Phi_{e,603}(D,\lambda)$ is scaled to $\Phi_{e,603}(\lambda)$ such that

$$k = \frac{\int \Phi_{e,603}(D,\lambda)\,d\lambda}{\int \Phi_{e,603}(\lambda)\,d\lambda}. \tag{7}$$

The normalized amount of emitted photons as a function of wavelength $\Phi_{e,603}(\lambda)$ is calculated from the normalized emission spectrum $E_n(\lambda)$.

The amount of emitted photons $\Phi_{e,603}(D,\lambda)$ then is added to the already modified AM1.5G spectrum $\Phi_{sa,603}(D,\lambda)$ with Eq. (2) to yield

$$\Phi_{sa\,e,603}(D,\lambda) = \Phi_{sa,603}(D,\lambda) + \Phi_{e,603}(D,\lambda). \tag{8}$$

The modified spectrum $\Phi_{sa\,e,603}(D,\lambda)$ serves as input for the solar cell simulation models.

As an example, Fig. 4 shows the result of this procedure for the QD with $\lambda_{em} =$ 603 nm, which also illustrates the effect of QD concentration. For a converter

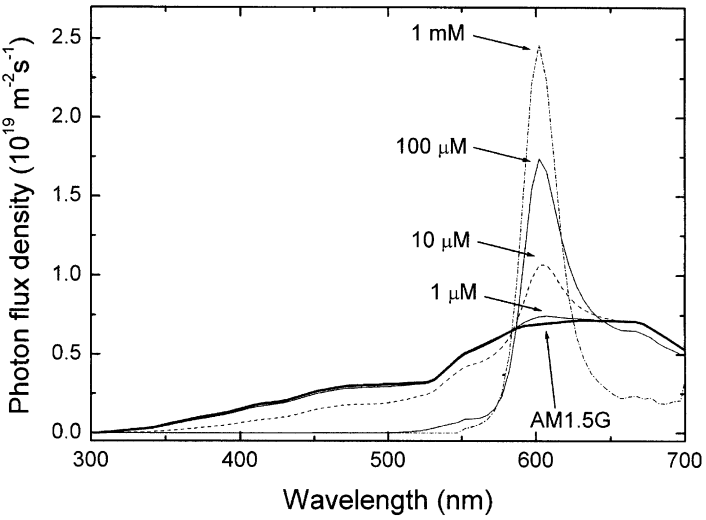

Fig. 4. Calculated modified spectra for various QD concentrations that notably influence the AM1.5G spectrum, i.e., 1,10, and 100 μM and 1 mM.

thickness $D = 1$ mm, we have varied the QD concentrations from 1 μM to 1 mM. At a concentration of 1 μM an appreciable amount of photons is absorbed in the blue part of the AM1.5G spectrum, while the modified spectrum is increased at the QD emission wavelength. For higher concentrations this effect is clearly much stronger. Note, that the product *CD* determines the amount of spectral change. Optimum values for QD concentration are related to the thickness of the converter.

In order to study the effect of different QD size we shifted the emission spectra in the emission wavelength range 300–700 nm, with 50 nm steps. We assumed that the form of spectra remains identical, which is reasonable, as seen in reported absorption/emission spectra as a function of QD size [36–41]. The particle diameters are again determined from the absorption maxima using the relation between absorption maximum and particle diameter reported in literature [39–41]. The extinction coefficients are then calculated with the equation from Leatherdale et al. [37]. The modified spectra $\Phi_{sa,\lambda_{em}}(D,\lambda)$ are calculated following the procedure described above.

3. Results and discussion

3.1. Small-band spectrum

The effect of incident small-band spectra on solar cell performance can be easily simulated. We varied the center emission wavelengths of the QDs in 50-nm steps in

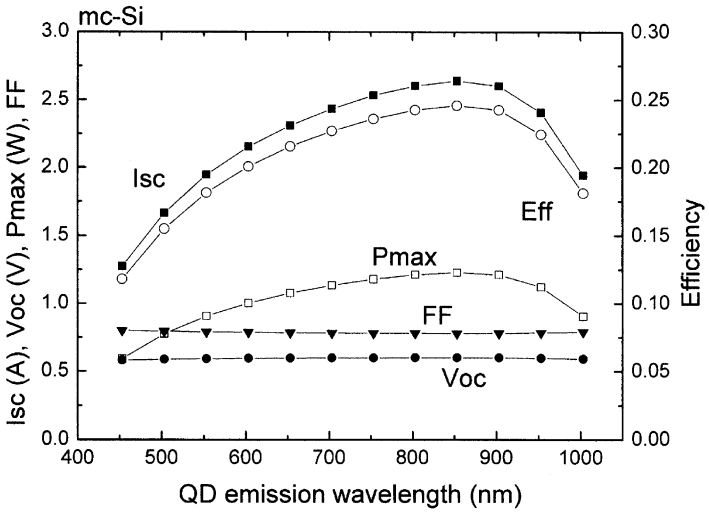

Fig. 5. Effect of small-band QD emission (500 W/m^2) on the parameters I_{sc}, V_{oc}, FF, P_{max}, and efficiency of the mc-Si solar cell as a function of center emission wavelength. Right-hand scale: I_{sc}, V_{oc}, and P_{max}, left-hand scale FF and efficiency.

the range 400–1000 nm, scaled to 500 W/m^2. The results obtained with PC1D for the mc-Si cell are shown in Fig. 5. A clear increase in short-circuit current from 1.3 A at QD emission wavelength of 453 nm to an optimum of 2.6 A at 853 nm is observed, with a concomitant increase in conversion efficiency from 12% to 24%. Both fill factor and open-circuit voltage hardly change. The optimum wavelength of 853 nm does not coincide with the wavelength where the spectral response is at its maximum (see Fig. 2b). At this optimum of about 600 nm the spectral response is 11% larger than the one at 850 nm. At present, we cannot explain this. The performance parameters compare most favorably to the ones obtained from simulation with an AM1.5G spectrum at 500 W/m^2 spectral density, i.e., short-circuit current $I_{sc} = 1.559$ A, open-circuit voltage $V_{oc} = 0.5851$ V, fill factor FF = 0.7937, efficiency $\eta = 14.48\%$. Clearly, if the complete AM1.5G spectrum could be converted to only one small-banded wavelength region the optimum center wavelength should be around 850 nm, which leads to a near doubling of conversion efficiency.

The effects on hydrogenated amorphous silicon solar cells are much less spectacular. The simulation results with ASA are shown in Fig. 6. Clearly, an optimum in short-circuit current exists at a QD emission wavelength of 500 nm, i.e., $I_{sc} = 55.63\,A/m^2$. This optimum coincides with the optimum in the spectral response curve (Fig. 2b). However, the optimum is lower than the short-circuit current calculated using the AM1.5G spectrum at 500 W/m^2 spectral density: $I_{sc} = 59.53\,A/m^2$. This most probably is caused by the small-banded spectral response of the a-Si:H cell.

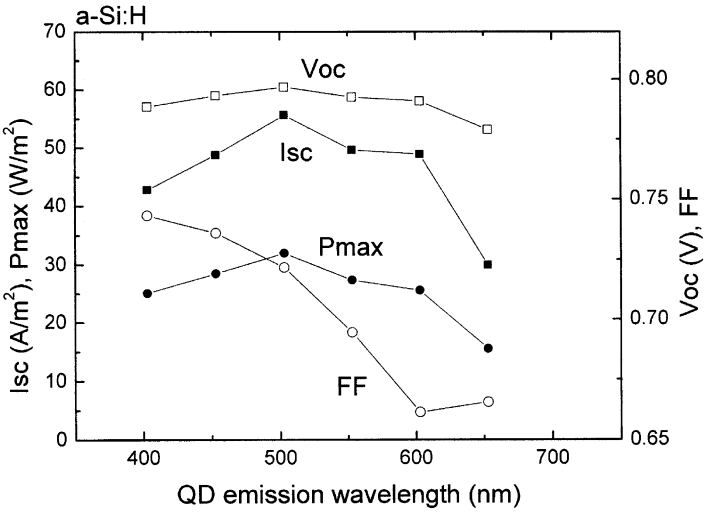

Fig. 6. Effect of small-band QD emission (500 W/m^2) on the parameters I_{sc}, V_{oc}, FF, and P_{max} of the a-Si:H solar cell as a function of center emission wavelength. Right-hand scale: I_{sc} and P_{max}, left-hand scale V_{oc} and FF.

3.2. Modified AM1.5G spectrum

As the optimum center emission wavelength of QDs in the planar converter on top of a mc-Si solar cell appears to be around 600 nm, we simulated the solar cell performance changes for the QDs with $\lambda_{em} = 603$ nm for a concentration range from 1 nM to 1 mM. The effects on the AM1.5G spectrum were already shown in Fig. 4 for a concentration range from 1 μM to 1 mM.

Fig. 7 shows IV characteristics of the mc-Si solar cell for the concentration range from 1 nM to 100 μM. A clear constant increase in short-circuit current of about 6×10^5%/M is observed up to a concentration of 1 μM. For higher concentrations the effect levels off, to even decrease at a concentration of 1 mM (not shown). Here, the beneficial effect is counteracted by the increased absorption due to this high concentration. The effect on all solar cell performance parameters is shown in Table 2. Clearly, the effects start to occur at 1 μM. While both short-circuit current and maximum generated power P_{max} follow similar behavior, the open-circuit voltage and fill factor only slightly decrease. Note that the efficiency in this table does not equal $FFI_{sc}V_{oc}$. As the QD concentration increases the spectral density incident on the solar cell decreases. We calculated the efficiency based on this decreasing intensity and not based on 1000 W/m^2. Therefore, the effect on efficiency is most spectacular: an increase of 30–40% is calculated.

It should be noted that in practice the results for the highest concentrations (0.1–1 mM) will not be as high as presented here, due to the fact that re-absorption is not taken into account in our simulations. This will lower the amount of emitted photons that enter the solar cell, which will be apparent in a lower peak in the

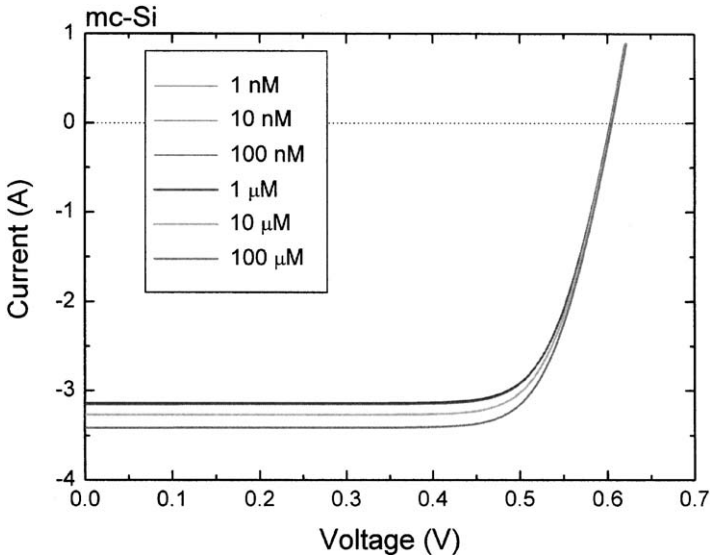

Fig. 7. The effect of QD concentration on the IV characteristics of the mc-Si solar cell.

Table 2
Solar cell performance parameters I_{sc}, V_{oc}, FF, P_{max}, and efficiency of the mc-Si solar cell with down converter layer as a function of QD concentration

QD concentration (μM)	I_{sc} (mA/cm^2)	V_{oc} (V)	P_{max} (W/m^2)	FF	Integrated spectrum (W/m^2)	η (%)
0	31.32	0.6029	14.55	0.7705	1000.0	14.55
0.001	31.32	0.6029	14.55	0.7705	1000.0	14.55
0.01	31.32	0.6029	14.55	0.7705	999.9	14.55
0.1	31.34	0.6029	14.56	0.7706	999.2	14.57
1	31.51	0.6031	14.63	0.7699	991.9	14.75
10	32.67	0.6040	15.16	0.7683	937.9	16.16
100	34.12	0.6051	15.82	0.7662	828.4	19.10
1000	33.75	0.6048	15.65	0.7667	780.1	20.06

modified spectrum at the QD emission center wavelength. Nevertheless, a relative increase of near 10% is to our opinion realizable. In addition, as the product of QD concentration and converter thickness *CD* determines the amount of spectral change, high concentrations can be avoided in converters of larger thickness, as long as *CD* remains constant.

For the simulation of QDs in the planar convertor on top of a-Si:H cells we used QDs of center emission wavelength of 503 nm, as at this wavelength the strongest effects are expected (Fig. 6). The results for the short-circuit current are shown in Table 3, for a concentration range from 0.1 μm to 10 mM. At about a concentration

Table 3
Solar cell performance parameters I_{sc}, V_{oc}, FF, P_{max}, and efficiency of the a-Si:H solar cell with down converter layer as a function of QD concentration

QD concentration (μM)	I_{sc} (mA/cm^2)	V_{oc} (V)	P_{max} (W/m^2)	FF	Integrated spectrum (W/m^2)	η (%)
0	11.92	0.8135	6.548	0.6752	1000.0	6.548
0.1	11.92	0.8135	6.547	0.6752	1000.0	6.548
1	11.91	0.8135	6.543	0.6753	999.9	6.547
10	11.85	0.8134	6.503	0.6747	994.3	6.547
100	11.38	0.8124	6.204	0.6711	959.7	6.540
1000	10.35	0.8102	5.620	0.6702	909.1	6.182
10000	9.274	0.8079	5.114	0.6826	875.7	5.840

of 10 μm the effects on short-circuit current start to be noticeable. This concentration is one order of magnitude higher than in the case of mc-Si. Also in contrast to mc-Si, here, the short-circuit current decreases with about 10% for a concentration of 1 mM, in close correspondence to the decrease in spectral intensity (Fig. 9). This has clearly to do with the amount of absorbed photons balanced with the emitted photons in relation to the spectral response. The aim of applying QDs as wavelength shifters is only sensible when an appreciable difference exists in spectral response between the QD center emission wavelength and the lower wavelengths. As the spectral response of the a-Si:H solar cell is already high at low wavelengths, beneficial effects, if any, will be small. Only when the QD quantum efficiency equals unity, and when in addition all emitted photons enter the solar cell, an increase in short-circuit current is observed of about 4% for a concentration of 1 mM. Either increasing η_{em} or η_t to unity still leads to a decreasing short-circuit current.

Experimental verification of the above results is in progress. To this end CdSe/ZnS core/shell QDs have been dispersed in a polymer at varying concentrations. We have selected a polylaurylmethacrylate (PLMA) matrix, of which it is reported that the quantum efficiency of QDs is retained after dispersion in PLMA [28]. Various QD/polymer solution were coated on top of microscope slide, and from their homogeneous color we infer that segregation does not occur.

4. Conclusion

The inclusion of a planar converter that contains wavelength-shifting moieties such as quantum dots allows for a better use of the solar spectrum. However, the most beneficial effects will be accomplished if the spectral response of solar cells has a specific form such that the spectral response is low at low wavelengths and high at high wavelengths. The wavelength-shifting moieties should shift the wavelengths where the spectral response is low to wavelengths where the spectral response is high. Further, losses associated with low quantum efficiency and isotropic emission should

be avoided, i.e., the quantum efficiency should be as high as possible (unity preferred) and internal reflection conditions should be optimized.

Here we demonstrated that QDs with a center emission wavelength of 603 nm included in a planar converter on top of a multi-crystalline solar cell are capable of increasing the short-circuit current by nearly 10%. A concomitant increase in efficiency, calculated with the amount of photons incident on the solar cell can be as high as 30–40%. Simulation results for planar converters on hydrogenated amorphous silicon solar cells show no beneficial effects, due to the high spectral response at low wavelength.

Acknowledgements

We gratefully acknowledge the fruitful discussions on QDs with Sander Wuister, Celso de Mello Donegá, and Cynthia Harkisoen (Utrecht University). Furthermore, we would like to thank the Netherlands Organization for Energy and the Environment (NOVEM) for financial support through their NEO programme (contract 0268-02-03-04-0002) and the European Commission for financial support as part of the Framework 6 integrated project FULLSPECTRUM (contract SES6-CT-2003-502620).

References

[1] M.A. Green, Solar Cells; Operating Principles, Technology and Systems Application, Prentice-Hall, Englewood Cliffs, NJ, USA, 1982.
[2] A. Luque, S. Hegedus (Eds.), Handbook of Photovoltaic Science and Engineering, Wiley, Chichester, UK, 2003.
[3] A. Luque, A. Marti, Phys. Rev. Lett. 78 (1997) 5014–5017.
[4] A.J. Chatten, K.W.J. Barnham, B.F. Buxton, N.J. Ekins-Daukes, M.A. Malik, Sol. Energy Mater. Sol. Cells 75 (2003) 363–371.
[5] T. Trupke, M.A. Green, P. Würfel, J. Appl. Phys. 92 (2002) 1668–1674.
[6] T. Trupke, M.A. Green, P. Würfel, J. Appl. Phys. 92 (2002) 4117–4122.
[7] M.A. Green, Third Generation Photovoltaics, Advanced Solar Energy Conversion, Springer, Berlin, Germany, 2003.
[8] A. Martí, A. Luque (Eds.), Next Generation Photovoltaics, High Efficiency through Full Spectrum Utilization, Institute of Physics Publishing, Bristol, UK, 2004.
[9] A. Luque, A. Martí, A. Bett, V.M. Andreev, C. Jaussaud, J.A.M. van Roosmalen, J. Alonso, A. Räuber, G. Strobl, W. Stolz, C. Algora, B. Bitnar, A. Gombert, C. Stanley, P. Wahnon, J.C. Conesa, W.G.J.H.M. Van Sark, A. Meijerink, G.P.M. Van Klink, K. Barnham, R. Danz, T. Meyer, I. Luque-Heredia, R. Kenny, C. Christofides, G. Sala, P. Benítez, Sol. Energy Mater. Sol. Cells (2005), this issue.
[10] A. Luque, A. Martí, Theoretical limits of photovoltaic conversion, in: A. Luque, S. Hegedus (Eds.), Handbook of Photovoltaic Science and Engineering, Wiley, Chichester, UK, 2003.
[11] R.E.I. Schropp, M. Zeman, Amorphous and Microcrystalline Silicon Solar Cells: Modeling, Materials, and Device Technology, Kluwer Academic Publishers, Boston, MA, USA, 1998.
[12] W.G.J.H.M. Van Sark, Methods of deposition of hydrogenated amorphous silicon for device applications, in: M.H. Francombe (Ed.), Thin Films and Nanostructures, vol. 30, Academic Press, San Diego, 2002, pp. 1–215.

[13] R.E.I. Schropp, private communication.
[14] R.L. Garwin, Rev. Sci. Instrum. 31 (1960) 1010–1011.
[15] W.H. Weber, J. Lambe, Appl. Opt. 15 (1976) 2299–2300.
[16] A. Goetzberger, W. Greubel, Appl. Phys. 14 (1977) 123–139.
[17] C.F. Rapp, N.L. Boling, in: Proceedings of the 13th Photovoltaic Specialists Conference, IEEE, Washington, DC, 1978, pp. 690–693.
[18] K. Barnham, J.L. Marques, J. Hassard, P. O'Brien, Appl. Phys. Lett. 76 (2000) 1197–1199.
[19] A.J. Chatten, K.W.J. Barnham, B.F. Buxton, N.J. Ekins-Daukes, M.A. Malik, in: Proceedings of the Third World Congress on Photovoltaic Energy Conversion (WPEC-3), pp. 2657–2660.
[20] A.P. Alivisatos, J. Phys. Chem. 100 (1996) 13226–13239.
[21] S.V. Gaponenko, Optical Properties of Semiconductor Nanocrystals, Cambridge University Press, Cambridge, UK, 1998.
[22] M. Bruchez Jr., M. Moronne, P. Gin, S. Weiss, A.P. Alivisatos, Science 281 (1998) 2013–2016.
[23] B.O. Dabbousi, J. Rodriguez-Viejo, F.V. Mikulec, J.R. Heine, H. Mattoussi, R. Ober, K.F. Jensen, M.G. Bawendi, J. Phys. Chem. B 101 (1997) 9463–9475.
[24] F.V. Mikulec, M. Kuno, M. Bennati, D.A. Hall, R.G. Griffin, M.G. Bawendi, J. Am. Chem. Soc. 122 (2000) 2532–2540.
[25] W.G.J.H.M. Van Sark, P.L.T.M. Frederix, A.A. Bol, H.C. Gerritsen, A. Meijerink, Chem. Phys. Chem. 3 (2002) 871–879.
[26] T. Maruyama, R. Kitamura, Sol. Energy Mater. Sol. Cells 69 (2001) 61–68.
[27] T. Maruyama, J. Bandai, J. Electrochem. Soc. 146 (1999) 4406–4409.
[28] J. Lee, V.C. Sundar, J.R. Heine, M.G. Bawendi, K.F. Jensen, Adv. Mater. 12 (2000) 1102–1105.
[29] R.T. Wegh, H. Donker, K.D. Oskam, A. Meijerink, Science 283 (1999) 663–666.
[30] J.M. Serin, D.W. Brousmiche, J.M.J. Frechet, J. Am. Chem. Soc. 124 (2002) 11848–11849.
[31] B.-C. Hong, K. Kawano, Sol. Energy Mater. Sol. Cells 80 (2003) 417–432.
[32] A. Polman, W.G.J.H.M. Van Sark, W.C. Sinke, F.W. Saris, Sol. Cells 17 (1986) 241–251.
[33] P.A. Basore, D.A. Clugston, in: Proceedings of the 25th IEEE Photovoltaic Specialists Conference, IEEE, Washington, DC, USA, 1996, pp. 377–381.
[34] P.A. Basore, D.A. Clugston, PC1D, User's Manual, Version 5.8, 2002.
[35] M. Zeman, J. van den Heuvel, M. Kroon, J. Willemen, Amorphous Semiconductor Analysis (ASA), User's Manual, Version 3.3, 2000.
[36] C. De Mello Donegá, S.G. Hickey, S.F. Wuister, D. Vanmaeckelbergh, A. Meijerink, J. Phys. Chem. B 107 (2003) 489–496.
[37] C.A. Leatherdale, W.-K. Woo, F.V. Mikulec, M.G. Bawendi, J. Phys. Chem. B 106 (2002) 7619–7622.
[38] O. Schmelz, A. Mews, T. Basché, A. Herrmann, K. Müllen, Langmuir 17 (2001) 2861–2865.
[39] C.B. Murray, D.J. Norris, M.G. Bawendi, J. Am. Chem. Soc. 115 (1993) 8706–8715.
[40] J.E. Bowen Katari, V.L. Colvin, A.P. Alivisatos, J. Phys. Chem. 98 (1994) 4109–4117.
[41] M. Jacobsohn, U. Banin, J. Phys. Chem. B 104 (2000) 1–5.